Available online at www.sciencedirect.com
SCIENCE DIRECT®
C. R. Mecanique 333 (2005) 694–698
COMPTES RENDUS MECANIQUE
http://france.elsevier.com/direct/CRAS2B/

Computational AeroAcoustics: from acoustic sources modeling to farfield radiated noise prediction

Study of stabilization methods for computational aeroacoustics

Ronan Guénanff, Marc Terracol

CFD & Aeroacoustics Department, ONERA – DSNA, BP 72, 29, avenue de la Division Leclerc, 92322 Châtillon cedex, France

Available online 8 September 2005

Abstract

The use of high-order centered finite difference to solve the Euler equations commonly requires a stabilization procedure. The present work is a theoretical analysis of these stabilization methods that make the whole algorithm (i) still consistent with the continuous problem and (ii) able to run long time simulations. In the present study, a theoretical analysis of the three commonly used methods resorting to the application of high-order filters is performed. An extension to non-periodic boundary conditions is studied to avoid numerical reflection and numerical instabilities due to the use of specific boundary schemes. ***To cite this article: R. Guénanff, M. Terracol, C. R. Mecanique 333 (2005).***

Résumé

Étude de méthodes de stabilisation en aéroacoustique numérique. La discrétisation des équations d'Euler par des différences finies centrées d'ordre élevé nécessite le recours à une procédure de stabilisation rendant l'algorithme discret (i) toujours consistant avec le problème continu et (ii) stable sur de longs temps de simulation. Cette étude propose une analyse théorique de trois méthodes de stabilisation recourant à l'application d'un filtre spatial d'ordre élevé sur la solution. Une extension aux conditions aux limites non-périodiques est étudiée pour éviter la réflection numérique et les instabilités numériques éventuelles dues à l'utilisation de schémas spécifiques aux limites du domaine de calcul. ***Pour citer cet article : R. Guénanff, M. Terracol, C. R. Mecanique 333 (2005).***

Keywords: Acoustics; Computational aeroacoustics; Stabilization method; Non-reflecting boundary condition

Mots-clés : Acoustique ; Aéroacoustique numérique ; Méthode de stabilisation ; Condition limite non réflechissante

1. Introduction

The finite-difference method is widely used to simulate acoustic wave propagation in flows. However, the definition of (i) stable and low-dispersive schemes and (ii) nonreflecting boundary conditions, remains an open problem.

* Corresponding author.
E-mail addresses: ronan.guenanff@onera.fr, ronan_guenanff@hotmail.fr (R. Guénanff), marc.terracol@onera.fr (M. Terracol).

1631-0721/$ – see front matter
doi:10.1016/j.crme.2005.07.015

An important point, which sustains the present work, is that the accuracy and efficiency of the global method depend on those of each element (numerical scheme, time integration method, boundary condition), but also on the way they interact. Another point is that, if industrial use is wanted, the method must be as general and as simple as possible.

A major drawback is the possible appearance and growth of high-frequency spurious modes when performing numerical simulations with this method. A way to prevent the growth of these modes is to resort to an additional step or an additional term in the numerical scheme that relies on adding numerical dissipation in the scheme. The procedure must take into account the discretization parameters. Among the usual approaches, we will study the artificial selective damping method [1] – or penalization method – and the application of a linear filter at the end of the time step [2].

2. Discretization of the linearized Euler equations

The perturbation Euler equations are generally used as mathematical model to describe acoustic waves propagation. The global unsteady field $U = [\rho, \rho u, E]^{\mathrm{T}}$ is splitted as the sum of a mean field $U_0 = [\rho_0, \rho_0 u_0, E_0]^{\mathrm{T}}$, and a fluctuating field $U_p = U - U_0 = [\rho_p, (\rho u)_p, E_p]^{\mathrm{T}}$, where ρ denotes density, u the velocity vector, and E the total energy. If we consider the hypothesis of some small perturbations around a steady mean flow $|U_p| = \mathrm{O}(\epsilon)|U_0|$, $\epsilon \ll 1$, then we obtain the Linearized Euler Equations (LEE) e.g. $((\rho u)_p = \rho u - \rho_0 u_0 \approx \rho_0 u_p + \rho_p u_0)$.

Under the assumption of a mean field verifying the Euler equations, the evolution equations of the fluctuating field are reduced to:

$$\frac{\partial U_p}{\partial t} + \nabla \cdot \big(\mathsf{F}(U_0 + U_p) - \mathsf{F}(U_0)\big) = 0 \tag{1}$$

where $\mathsf{F}(U)$ is the convective flux vector:

$$\mathsf{F}(U) = \begin{pmatrix} \rho u \\ \rho u \otimes u + p\,\mathrm{Id} \\ (\rho E + p)u \end{pmatrix} \tag{2}$$

with p the pressure and Id the identity matrix. The perfect gaz state-law makes it possible to close the system.

To obtain the Linearized Euler Equations, only terms in O(1) and O(ϵ) are kept.

From a numerical point-of-view, the sixth-order accurate centered finite-difference scheme is one of the most commonly used schemes in Computational AeroAcoustics (CAA) to discretize the spatial derivatives present in F.

This schemes can be expressed:

$$\frac{\partial f}{\partial x} \approx \frac{1}{\Delta x} \sum_{j=-3}^{3} a_j f(x + j\Delta x) \tag{3}$$

where the coefficients a_j are obtained by a high-order Taylor series expansion.

By applying the spatial Fourier transform, it becomes:

$$\mathrm{i}k\hat{f}(k) \approx \frac{1}{\Delta x} \sum_{j=-3}^{3} a_j\, \mathrm{e}^{jk\Delta x} \hat{f}(k) \tag{4}$$

In order to perform a theoretical study of the use of these schemes, we will consider the simplified case of the linear advection case with periodicity boundary conditions. The semi-discrete mono-dimensional advection problem at velocity c verifies, for the Fourier mode k:

$$\frac{\partial \hat{u}_k}{\partial t} = -\frac{c}{\Delta x}\mathrm{i} \cdot \left(\sum_{j=1}^{3} a_j \sin(jk\Delta x)\right)\hat{u}_k = -\frac{c}{\Delta x}\bar{k}(k)\hat{u}_k \tag{5}$$

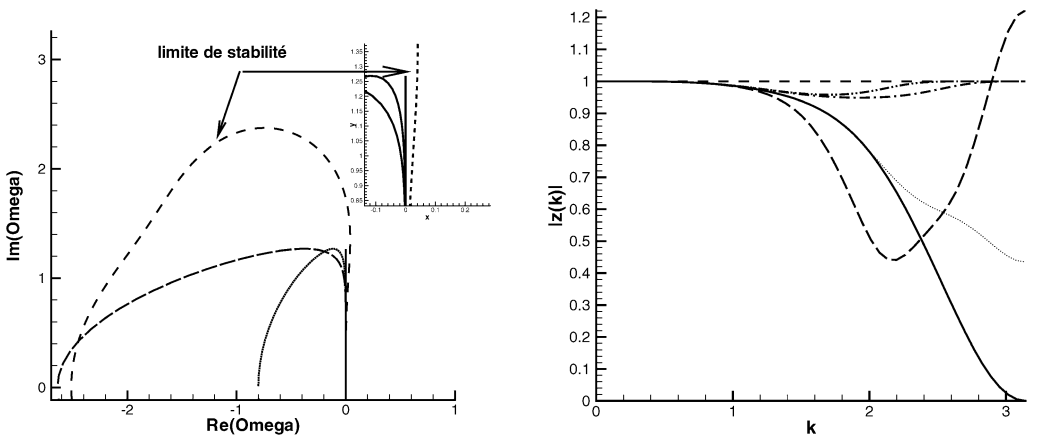

Fig. 1. Left, location of the eigenvalues of the Fourier modes: RK3 stability limit (dashed), $\overline{\Omega}(k) = c\Delta t\bar{k}(k)$ with $CFL = 0.8$ model 1 (solid) model 2 $\chi = \frac{1}{\Delta t}$ (dotted) $\chi = \frac{3.2}{\Delta t}$ (long dash). Right, amplification factor of the model: stability limit (dashed) basic model (---), model 1 (-·--), model 2 $\chi = \frac{1}{\Delta t}$ (dotted), $\chi = \frac{3.2}{\Delta t}$ (long dash), model 3 (solid).

Fig. 1. A gauche, localisation des valeurs propres des modes de Fourier : limite de stabilité du schéma RK3 (trait discontinu), $\overline{\Omega}(k) = c\Delta t\bar{k}(k)$ avec $CFL = 0{,}8$ modèl 1 (trait plein), modèle 2 $\chi = \frac{1}{\Delta t}$ (pointillés), $\chi = \frac{3.2}{\Delta t}$ (trait discontinu long). A droite, facteur d'amplification du modèle : limite de stabilité (trait discontinu), schéma de base (---), modèle 3 (trait plein).

The eigenvalue linked to this mode is purely imaginary for any k. The method is stable if and only if all the eigenvalues corresponding to the mode k from the grid lie in the stability domain of the temporal method. In this study, the explicit three-step third-order accurate Runge–Kutta scheme – with a rather large stability domain – will be considered.

For this algorithm, the location of the eigenvalues is the imaginary axis. The theoretical stability limit has thus to be taken on this axis and is equal to $\sqrt{3}/(\bar{k}(k_{\max}))$ where $k_{\max}$ leads to the maximum value of $\bar{k}(k) = \mathrm{i}\sum_{j=1}^{3} a_j \sin(jk\Delta x)$, $k \in [0, \pi/\Delta x]$. The extension to waves propagation in two or three dimensions in a medium at rest is then straightforward. For instance, in two dimensions, we have: $\overline{k_{2\mathrm{D}}}(k_x, k_y) = \pm \mathrm{i}c_0(\bar{k}(k_x)^2 + \bar{k}(k_y)^2)^{1/2}$ where c_0 denotes sound velocity. The complex number $\overline{k_{2\mathrm{D}}}$ thus remains purely imaginary, and the limit of stability is given by the maximum of $|\overline{k_{2\mathrm{D}}}|$.

High frequency modes are thus not damped and can lead to numerical instabilities. It is seen on Fig. 1 that the (O_y) axis is a limit of stability of the Runge–Kutta scheme.

3. Stabilization procedures

The following stabilization procedures both use a high-order spatial average operator $\mathcal{F}$ that cancel two points per wavelength modes [2,3]. They differ by the location of the filter application in the numerical algorithm:

– Model 1:

$$\frac{\partial U_i}{\partial t} = -\mathcal{F}\Big(\sum_{j=1,3} D_j \cdot \mathsf{F}_j(U_i)\Big)$$

– Model 2:

$$\frac{\partial U_i}{\partial t} = -\sum_{j=1,3} D_j \cdot \mathsf{F}_j(U_i) - \chi(\mathcal{F} - \mathrm{Id})(U_i)$$

– Model 3:

$$\begin{cases} \dfrac{\partial U_i}{\partial t} = -\left(\displaystyle\sum_{j=1,3} D_j \cdot \mathsf{F}_j(U_i) \right) \\ U^{n+1} = \mathcal{F} U^{n+1} \end{cases}$$

with D_j, the discrete derivation operator in the j direction and F_j, the jth column of the flux matrix.

We consider the particular framework of the mono-dimensional advection equation with speed c and periodic boundary conditions. The location of eigenvalues from both algorithms are to be compared with the one of the classical algorithm, that is the imaginary axis (Fig. 1). This analysis is not possible for model 3 in which time discretization is involved.

The results in Fig. 1 show that model 1 only allows one to work at a slightly larger CFL, because the maximum of the $\bar{k}$ function is lower than that of the classical algorithm. However, this model does not damp high-frequency spurious modes.

In model 2, a parameter χ is introduced that must be fixed as a function of the space-time discretization. When $\chi = 0$, the model is equivalent to the basic model. For a stable time integration, this parameter must be bounded. A nonzero real part appears in the eigenvalues obtained with this model. The stability of this procedure also depends on the stability limit of the temporal method on the real axis that is approximately (-2.5) (Fig. 1). If we denote $\chi = \frac{\alpha}{\Delta x}$, then one can write $0 < \frac{\alpha \Delta t}{\Delta x} = \chi \Delta t < 2.5$, or $\chi < \frac{2.5}{\Delta t}$. For a convenient value of χ, this method does thus damp high-frequency spurious modes (Fig. 1) .

The analysis of the amplification factor of the third-order Runge–Kutta method allows one to classify the three models. In Fig. 1, it is clear that model 2 with $\chi = \frac{1}{\Delta t}$ is stable while the value $\chi = \frac{3.2}{\Delta t}$ leads to an unstable numerical scheme. Model 3, where the filtering is applied at the end of the iteration, does not exhibit this drawback (Fig. 1). With this model, the amplification factor of the numerical scheme is zero for the mode with two points per wavelength and vanishes for high-frequencies. Model 3 is retained for the following tests.

4. Extension to nonreflecting boundary conditions

The Fourier analysis is no longer valid for boundary conditions modelling waves leaving the computational domain. One can thus resort to matrix analysis [4]. This method analyses the effect of both spatial numerical scheme and boundary conditions thanks to the construction of a closed system of linear differential equations. The hypothesis of an exact temporal integration makes the reconstruction of the solution possible via the eigenvalues and eigenvectors of the system.

The exit boundary condition studied here consists in the decrease of the spatial operators order – derivation and filtering – in a sponge zone adjacent to the boundary [5]. The use of noncentered operators, that can lead to numerical instabilities, is thus avoided.

The order of the spatial filter decrease from ten to two in the five ghost points – introducing a strong dissipation for outgoing waves – and the order of the differentiation operator from six to two – leading to a strong dispersion for outgoing waves. At the last ghost point, a homogeneous Dirichlet boundary condition is applied. These five ghost points constitute a layer which absorbs the energy. The following remarks relative to the analysis of the eigenvalues and the eigenvectors of the system can be made. The location of the eigenvalues (not presented here) proves that the model is stable. Two types of eigenvectors appear (Fig. 2): (i) spurious eigenvectors with high frequencies contributions corresponding to eigenvalues with a strongly negative real part – fast decaying in time – and (ii) eigenvectors with a zero contribution inside of the domain corresponding to eigenvalues with a real part close to zero that make the waves leave the computational domain. As a consequence, the method is revealed to be stable and nonreflecting.

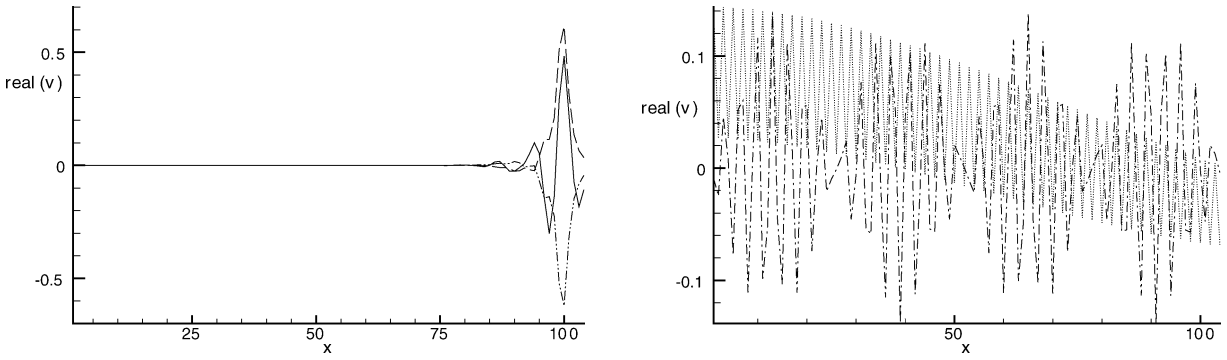

Fig. 2. Matrix analysis of model 3 with exit waves boundary conditions. Examples of some eigenmodes with a real part corresponding to sustained modes (left), $\mathrm{Re}(\lambda_i) \approx 0$ and fast decaying modes $\mathrm{Re}(\lambda_i) \ll 0$ (right).

Fig. 2. Analyse matricielle du modèle 3 avec des conditions aux limites de sortie des ondes. Exemples de modes propres avec une partie réelle correspondant à un mode soutenu (gauche), $\mathrm{Re}(\lambda_i) \approx 0$, et modes à décroissance rapide $\mathrm{Re}(\lambda_i) \ll 0$ (droite).

5. Conclusion

The numerical analysis of stabilization methods for central finite difference schemes performed in this work has shown its major effect on the global numerical method. A bound for the relaxation parameter of the penalization method was derived corresponding to a new stability limit characteristic of the time integration method. The method which consists in the application of a linear filter at the end of the time step appears to be the most appropriate for the stabilization, with a stability limit driven only by the CFL number. An extension of this method for non-periodic cases has been studied. The method is revealed to be stable and nonreflecting. Additional simulations, not presented here for sake of briefness, were successfully performed [6], simulating the exit of mono-dimensional and bidimensional acoustic waves.

Acknowledgements

The authors would like to acknowledge Professor R. Lewandowski, Professor P. Sagaut and Doctor E. Manoha for useful discussions.

References

[1] C.W.K. Tam, Computational aeroacoustics: issues and methods, AIAA J. 33 (10) (1995) 1748.
[2] D.V. Gaitonde, J.S. Shang, J.L. Young, Practical aspects of high-order numerical schemes for wave propagation phenomena, Int. J. Numer. Methods Engrg. 45 (1999) 1849.
[3] S. Lele, Computational aeroacoustics: a review, AIAA Paper 97-0018, 1997.
[4] C. Hirsch, Numerical Computation of Internal and External Flows, J. Wiley & Sons, New York, 1988.
[5] S. Redonnet, E. Manoha, P. Sagaut, Numerical Simulation of propagation of small perturbations acting with flows and solid bodies, AIAA Paper 2001-2223, 2001.
[6] R. Guénanff, M. Terracol, E. Manoha, P. Sagaut, Theoretical and numerical aspects of a high-order multi-domain method for CAA, AIAA Paper 2003-25090, 2003.